Wide-Band Unambiguous Quantum Sensing via Geodesic Evolution

Ke Zeng,[1] Xiaohui Yu,[1] Martin B. Plenio,[2] and Zhen-Yu Wang[1,3,*]
[1]Key Laboratory of Atomic and Subatomic Structure and Quantum Control (Ministry of Education), Guangdong Basic Research Center of Excellence for Structure and Fundamental Interactions of Matter, School of Physics, South China Normal University, Guangzhou 510006, China
[2]Institut für Theoretische Physik und IQST, Universität Ulm, Albert-Einstein-Allee 11, 89081 Ulm, Germany
[3]Guangdong Provincial Key Laboratory of Quantum Engineering and Quantum Materials, and Guangdong-Hong Kong Joint Laboratory of Quantum Matter, South China Normal University, Guangzhou 510006, China

(Received 20 July 2023; accepted 21 May 2024; published 20 June 2024)

We present a quantum sensing technique that utilizes a sequence of π pulses to cyclically drive the qubit dynamics along a geodesic path of adiabatic evolution. This approach effectively suppresses the effects of both decoherence noise and control errors while simultaneously removing unwanted resonance terms, such as higher harmonics and spurious responses commonly encountered in dynamical decoupling control. As a result, our technique offers robust, wide-band, unambiguous, and high-resolution quantum sensing capabilities for signal detection and individual addressing of quantum systems, including spins. To demonstrate its versatility, we showcase successful applications of our method in both low-frequency and high-frequency sensing scenarios. The significance of this quantum sensing technique extends to the detection of complex signals and the control of intricate quantum environments. By enhancing detection accuracy and enabling precise manipulation of quantum systems, our method holds considerable promise for a variety of practical applications.

DOI: 10.1103/PhysRevLett.132.250801

Introduction.—Accurate characterization of the qubit environment holds significant importance across a range of applications, spanning from quantum information processing to quantum sensing [1–4]. A widely utilized technique for achieving this is the implementation of dynamical decoupling (DD) pulse sequences [5,6]. These sequences serve to filter out environmental noise, thereby extending the quantum coherence time, as well as to extract and amplify signals of specific frequencies [3,4,7]. Consequently, qubits under such sequences become highly sensitive quantum sensors, presenting diverse applications. For instance, nitrogen-vacancy (NV) centers [8–10] subjected to DD pulse sequences enable nanoscale nuclear magnetic resonance (NMR) [7,11–27], spin label detection [28–30], spin cluster imaging [31–39], and ac field sensing [40–51]. Furthermore, they can be employed for controlling nearby single nuclear spins [52–57] in the context of quantum information processing [58,59], quantum simulations [60], and quantum networks [61–64].

However, DD pulse sequences used for quantum sensing, such as the commonly employed Carr-Purcell-Meiboom-Gill (CPMG) [65,66] and XY8 [67] sequences encounter an issue known as spectral leakage and spurious resonance. These complications make the interpretation of the sensor's recorded signal challenging and can result in ambiguous signal identification [68,69]. DD pulses introduce abrupt temporal state flipping of the qubit sensor, causing a pronounced frequency modulation at a specific frequency [indicated by the gray line in Fig. 1(d)]. This modulation leads to a strong resonance when the flipping frequency ω matches the signal frequency ν, i.e., $\omega = \nu$, enabling frequency-selective sensing. However, it also generates resonances at other harmonic frequencies $\omega = \nu/k$ $(k = 3, 5, 7, \ldots)$, as evident in its Fourier transform [represented by the gray squares in Fig. 1(d)]. On the other hand, the limited power of control pulses further introduces spurious signals at unexpected frequencies, $\omega = s\nu/k$ with $s \in \{2, 4, \ldots\}$ [68]. Moreover, quantum heterodyne methods employed to down-convert high-frequency signals for sensing can exacerbate signal overlap [48–50]. These factors collectively present obstacles to reliably measuring environmental signals, particularly when various background noise sources are not fully characterized. With this goal in mind, sequence timing has been optimized [70,71] to eliminate low harmonics (e.g., $k = 3$) and sequence randomization has been explored to mitigate spurious signals (i.e., $s \neq 1$) [72,73]. However, both approaches can address only specific their aspects and can solve these only partially. Obtaining a universal method to address these problems (e.g., by numerical optimization algorithms) is challenging considering the unavoidable control errors and the unknown, potentially quantum, environment, as well as the demanding computing resources.

In this Letter, we present a novel approach called cyclic geodesic driving to solve these problems, enabling unambiguous sensing of signals across a broad frequency range

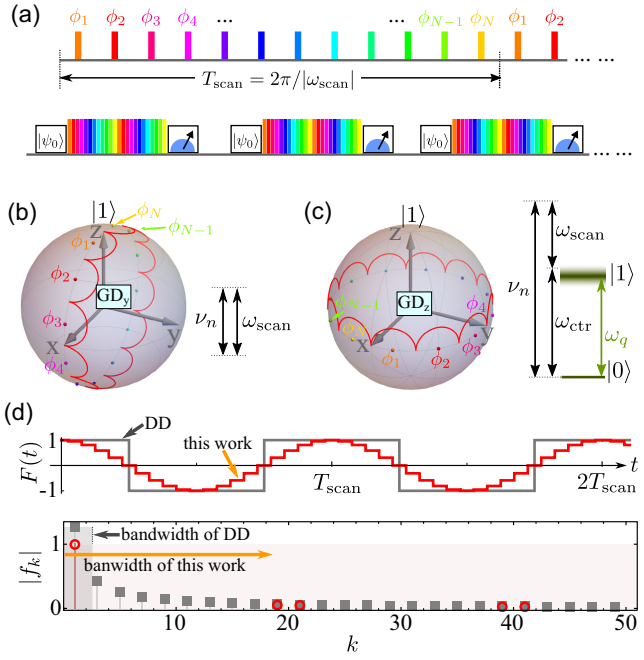

FIG. 1. Quantum sensing via geodesic jumping. (a) Upper panel: repeated application of a sequence of N π pulses realizes cyclic quantum adiabatic evolution along the geodesic in (b) or (c). Lower panel: combined with synchronized readout techniques for arbitrary frequency resolution. (b) GD$_y$, where the closed geodesic is sampled by N π pulses. The red solid line illustrates the trajectory of the state evolution starting at $|1\rangle$ for $N = 12$. When $\omega_{\rm scan}$ matches the frequency ν_n of the target, a resonance occurs. (c) As (b) but for GD$_z$ which uses a horizontal geodesic, e.g., for robust heterodyne sensing of high-frequency signal. The resonant condition is accurately tuned by $T_{\rm scan}$ and the frequency $\omega_{\rm ctr}$ of control field. (d) The resulting modulation function $F(t)$ (red line for $N = 20$) and its Fourier components (red cycles) where $f_k = 0$ for all $1 < k < N - 1$. The gray line and squares are the corresponding ones for DD pulse sequences.

on qubit sensors. Our method involves the application of a sequence of π pulses to implement accelerated high-fidelity quantum adiabatic driving, effectively inducing periodic evolution of the quantum sensor along the geodesic path on the Bloch sphere. As a result, the resonance frequency of the quantum sensor aligns with the frequency of the periodic evolution, while simultaneously mitigating the impact of environmental background noise. By employing this technique, each individual frequency signal generates a single, distinct signal response within the wide frequency band. This eliminates undesirable signal overlap, enabling precise characterization of complex external environments and signals. Our approach can be applied to more complex quantum sensing problems. For example, we show that it can be combined with the idea of signal frequency down-conversion [48–50] and can be combined with synchronized readout techniques [44,45] for achieving arbitrary high frequency resolution. Furthermore, our approach exhibits remarkable resilience against control errors, as it is the counterpart of quantum adiabatic control. Overall, our proposed method of cyclic geodesic driving offers a robust and effective solution for wide-band, unambiguous signal sensing, enabling accurate analysis of intricate quantum systems and external environments.

Adiabatic shortcut by jumping.—Our sensing scheme utilizes a sequence of periodic π pulses [Fig. 1(a)] which achieves cyclic quantum adiabatic evolution along a geodesic [74–77] defined by the control Hamiltonian for the qubit sensor

$$H_c(t) = \frac{E(t)}{2}(|+_\phi\rangle\langle+_\phi| - |-_\phi\rangle\langle-_\phi|), \tag{1}$$

where the instantaneous eigenstates $|\pm_\phi\rangle$ are varied by a parameter $\phi = \phi(t)$ starting with $\phi(0) = 0$ at the initial time $t = 0$. In the quantum adiabatic approximation, the evolution operator takes the form [74,78,79]

$$U_c(\phi) = e^{-i\varphi_+(t)}|+_\phi\rangle\langle+_0| + e^{-i\varphi_-(t)}|-_\phi\rangle\langle-_0|, \tag{2}$$

which transfers the initial state $|\pm_0\rangle$ to the instantaneous eigenstate $|\pm_\phi\rangle$ at a later time. We use the Born-Fock gauge $\langle\pm_\phi|(d/d\phi)|\pm_\phi\rangle = 0$ such that $\varphi_\pm(t) = \pm\frac{1}{2}\int_0^t E(t')dt'$ are the dynamic phases. To realize the adiabatic evolution $U_c(\phi)$ by $H_c(t)$ with high fidelities in finite times, we choose

$$\begin{aligned}|+_\phi\rangle &= \cos\left(\frac{\phi}{2}\right)|+_0\rangle + \sin\left(\frac{\phi}{2}\right)|-_0\rangle,\\ |-_\phi\rangle &= -\sin\left(\frac{\phi}{2}\right)|+_0\rangle + \cos\left(\frac{\phi}{2}\right)|-_0\rangle,\end{aligned} \tag{3}$$

which connect two orthonormal states $|\pm_0\rangle$ via a geodesic curve [80]. In our scheme we apply a sequence of control π pulses via Eq. (1) with $\phi = \phi_j$ at the moments $T_j = T_{\rm scan}[(2j-1)/2N]$ $(j = 1, 2, \ldots)$, where N is the pulse number in one periodic of evolution, see Fig. 1(a). We use the linear relation $\phi_j = \omega_{\rm scan}T_j$, where frequency $\omega_{\rm scan}$ can be negative or positive depending on the change of ϕ_j in time. Each control π pulse has a time duration t_j such that the pulse area $\int_{T_j-t_j/2}^{T_j+t_j/2} E(t)dt = \pi$. Between the π pulses, there is no control, i.e., $E(t) = 0$ if $\phi \notin \{\phi_j\}$. We remove the dynamic phases at the final time of the evolution; we introduce a π phase shift to the pulses in the second-half of the sequence. According to Refs. [74–76], the sequence realizes $U_c(\phi)$ with unit fidelity at the middle of any successive path points $\phi = \bar{\phi}_j \equiv (\phi_{j+1} + \phi_j)/2$. For other values of $\phi \notin \{\bar{\phi}_j\}$, the difference between $U_c(\phi)$ and the actual evolution implemented by $H_c(t)$ is negligible when N is sufficiently large. See Figs. 1(a) and 1(b) for how the evolution of an initial eigenstate follows the path defined by the directions of successive π pulses (i.e., by the eigenstates

of the π pulse control). In contrast to conventional shortcuts to adiabaticity [79] to accelerate the adiabatic process, in our method the instantaneous eigenstates of the control Hamiltonian $H_c(t)$ are the same as the evolution path $|\pm_\phi\rangle$ in Eq. (2). This avoids the use of counterdiabatic fields and retains the intrinsic robustness of a traditional adiabatic process [76].

Unambiguous wide-bandwidth robust sensing.—To demonstrate the concept of quantum sensing through the aforementioned geometric control, we examine a qubit coupled to its environment via the interaction Hamiltonian

$$H_{\rm int}(t) = \frac{1}{2}\sigma_z B(t), \tag{4}$$

where the Pauli operator $\sigma_z = |1\rangle\langle 1| - |0\rangle\langle 0|$ and $B(t)$ could be a classical field or a quantum operator in a rotating frame which includes possible dephasing noise. We use the control Hamiltonian $H_c(t) = \Delta(t)(\sigma_z/2) + \Omega(t)(\sigma_x/2)$ and the states $|+_0\rangle = |1\rangle$ and $|-_0\rangle = |0\rangle$ for the geodesic in Eq. (3) for sensing. This geodesic driving around the y axis (GD_y) is sketched in Fig. 1(b). In the rotating frame of $H_c(t)$, $H_{\rm int}(t)$ becomes $\tilde{H}_{\rm int}(t) \approx \frac{1}{2} U_c^\dagger \sigma_z U_c B(t)$. For the evolution Eq. (2), we find the approximated transformations [81]

$$U_c^\dagger \sigma_z U_c \approx \cos\phi\sigma_z; \quad U_c^\dagger \sigma_x U_c \approx \sin\phi\sigma_z; \quad U_c^\dagger \sigma_y U_c \approx 0, \tag{5}$$

which have the nice property that they only depend on the geometric parameter $\phi(t)$. We obtain [81]

$$\tilde{H}_{\rm int}(t) \approx F(t)\frac{\sigma_z}{2} B(t). \tag{6}$$

When the number of pulses N is sufficiently large, the modulation function $F(t) \approx \cos(\omega_{\rm scan} t)$ has only one Fourier component over a large frequency band, see Fig. 1(d). Conventional DD sequences [3,4] also induce modulation factors $F(t)$ to the σ_z operator with $F(t) \in \{\pm 1\}$ for ideal sequences [3,4,85]. However, those modulation factors have multiple Fourier components that complicate the interpretation of the sensor's signal [68–70], see Fig. 1(d) for equally spaced DD sequences [3,4,65–67,86–88].

In Figs. 2(a)–2(d) we simulate the measured spectrum of a classical ac field with $B(t) = \sum_{j=1}^{3} b_j \cos(\nu_j t + \theta_j)$, where ν_j are the frequencies of different components. For the result of Fig. 2(a) obtained by the widely used robust XY8 sequence with an interpulse duration τ [67], all the frequencies ($\{\nu_j/2\pi\} = \{500, 1500.05, 2499.88\}$ kHz) cause transitions of the sensor states at $1/(2\tau) \approx 500$ kHz via the first, third, and the fifth harmonics. This problem of ambiguous spectral overlap is not solved even when we improve the frequency resolution sufficiently high via the synchronized readout technique (Qdyne) [44,45], see Fig. 2(c), because all the frequency components contribute to the readout signal in Qdyne. However, using GD_y, only

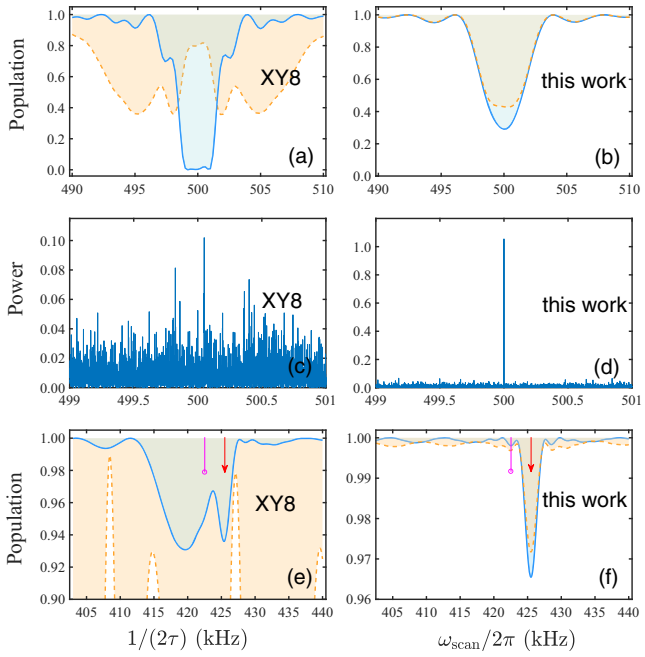

FIG. 2. Quantum spectroscopy. (a) Population signal of XY8 sequence (blue solid line) for spectroscopy of ac fields with the frequencies $\{\nu_j/2\pi\} = \{500, 1500.05, 2499.88\}$ kHz by varying the pulse interval τ. The 1500.05 kHz and 2499.88 kHz ac fields distort the signal centered at 500 kHz via the third and fifth harmonics, respectively. Yellow dashed line is the result when there is dephasing noise (with a control-free decoherence time $T_2^* \approx 2$ μs) and control errors (with about 20% drift on the amplitude of control field). (b) As (a) but by using GD_y. The 500 kHz signal dip is not distorted by the 1500.05 kHz and 2499.88 kHz ac fields. (c) Power spectrum for the ac signal fields in (c) by using the synchronized readout technique in Refs. [44,45]. The resonances due to higher harmonics make the signal unidentifiable even through the expected spectral resolution is about 1 Hz. (d) As (c) but by using GD_y. (e) Signal of XY8 sequence for the detection of a ^{1}H spin with its frequency indicated by a red arrow. The spurious resonance (centered around the pink vertical line) produced by a ^{13}C spin in diamond distorts the ^{1}H spin signal. Yellow dashed line is the result when there is a $2\pi \times 2$ MHz detuning error and 30% of amplitude drift in the control field. (f) As (e) but by using GD_y, where the spurious signals disappear. See [81] for details of the simulation.

the frequency $\nu_1/2\pi = 500$ kHz contributes to the dip at the resonance $\omega_{\rm scan} = \nu_1$, because we have the effective Hamiltonian $\tilde{H}_{\rm int} \approx \frac{1}{4} b_1 \cos\theta_1 \sigma_z$ from Eq. (6) after the rotating wave approximation [81]. The phase dependence on the effective Hamiltonian (and hence the signal) allows for arbitrary frequency resolution with synchronized readout, see Figs. 2(d) and 1(a). The results also show that our protocol is more resistant to control errors and dephasing noise. The already strong robustness of GD_y is enhanced further with an increasing number N of pulses, see Fig. 4.

It is interesting that cyclic geodesic driving also fully solves the problems of spurious response due to

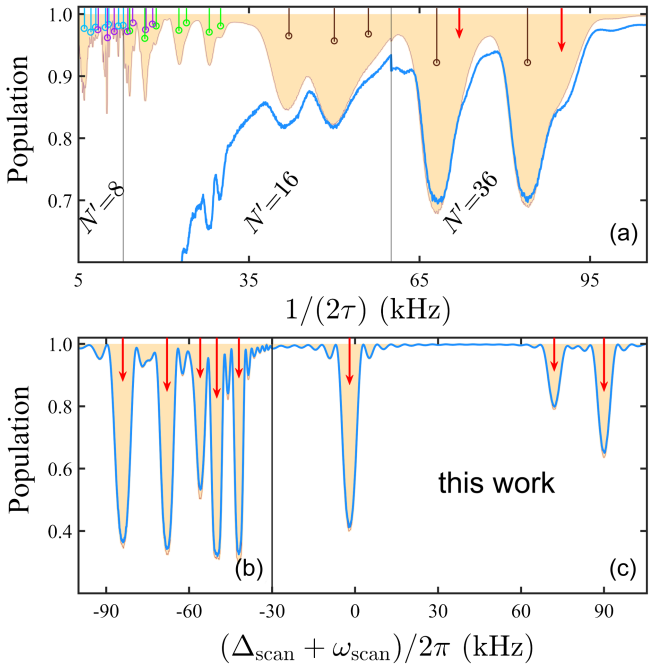

FIG. 3. (a) Quantum heterodyne spectroscopy of a signal field with frequencies $\{\nu_j\} = \omega_{\rm ctr} + 2\pi \times \{-84, -68, -56, -50, -42, -2, 72, 90\}$ kHz by using the protocol in Refs. [48,49] with the CPMG sequences. The blue solid line (the line with yellow filling) is the simulation with (without) dephasing noise that induces a control-free decoherence time $T_2^* \approx 2$ μs. The pulse interval τ is varied to measure the spectrum. Because for each ac signal frequency ν_j resonance dips occur whenever $1/(2\tau) = (\nu_j - \omega_{\rm ctr})/(2\pi k)$, $(k = \pm 1, \pm 3, \pm 5, \ldots)$, the true dips at $1/(2\tau) = (\nu_j - \omega_{\rm ctr})/(2\pi)$ indicated by red vertical arrows are obscured by other resonance dips (vertical lines). Different number N' of π pulses are used for different range of τ to insure that the sequence times are smaller than 1 ms. (b) [(c)]: As (a) but by using GD_z with fixed $\Delta_{\rm scan} = 0$ ($\omega_{\rm scan} = 2\pi \times 80$ kHz). All the dips only appear at the right frequencies ν_j. See [81] for details of simulation.

finite-width pulses [68], as detailed in [81]. In Figs. 2(e) and 2(f), we simulate the quantum sensing of a single proton spin (^{1}H) by an NV center. A ^{13}C spin in diamond is also coupled to the NV center as a noise source. For this case $B(t)$ is a quantum operator [53,54,81]. For the result Fig. 2(e) obtained by XY8 sequences, the spurious response from the ^{13}C spin disturbs the target proton spin signal and leads to misidentification of ^{13}C nuclei for proton. On the contrary, GD_y provides a clean signal dip in the spectrum [Fig. 2(f)], because when $\omega_{\rm scan}$ matches the frequency ν_1 of the target ^{1}H, $\tilde{H}_{\rm int} \approx \frac{1}{2} a_1^x \sigma_z I_1^x$ (where I_1^x is the ^{1}H spin operator and a_1^x is the hyperfine strength [81]) and the effect of the ^{13}C spin is removed.

Unambiguous heterodyne sensing.—The idea can be generalized to other settings. Consider the sensing of a multifrequency signal field $\vec{B}(t) = (B_x, B_y, B_z)$ with frequencies ν_j much larger than the Rabi frequency of the control field. We use GD_z [see Fig. 1(c)] with $|\pm_0\rangle = (|0\rangle \pm |1\rangle)/\sqrt{2}$ for the geodesic in Eq. (3) to sense the traverse part $B_\perp(t) \equiv B_x + iB_y = \sum_j b_j e^{i\alpha_j} \cos(\nu_j t + \theta_j)$. The relevant Hamiltonian reads

$$H = \frac{1}{2}(\omega_q + \delta_t)\sigma_z + \left(\frac{1}{2} B_\perp(t)\sigma_+ + \mathrm{H.c.}\right) + H_{\rm ctr},$$

where ω_q is the frequency of the qubit and δ_t is an unknown fluctuation. For NV qubits, ω_q (e.g., $\omega_q = D + \gamma_e B_z$ with $D = 2\pi \times 2.87$ GHz and $\gamma_e \approx 2\pi \times 2.8$ MHz/G) can be adjusted by changing the magnetic field B_z. The control Hamiltonian $H_{\rm ctr} = \Omega(t)\cos(\omega_{\rm ctr} t + \phi)\sigma_x$ has a controllable detuning $\Delta_{\rm scan} = \omega_{\rm ctr} - \omega_q$. In the rotating frame with respect to $\frac{1}{2}(\omega_q + \delta_t)\sigma_z + H_{\rm ctr}$, we obtain the effective interaction [81]

$$\tilde{H}_{\rm int}(t) \approx \frac{1}{4}\sum_j b_j e^{i(\alpha_j - \theta_j) + i(\omega_{\rm ctr} + \omega_{\rm scan} - \nu_j)t}\sigma_+ + \mathrm{H.c.} \quad (7)$$

Under the resonance condition for a signal frequency $\omega_{\rm ctr} + \omega_{\rm scan} = \nu_n$ and when $b_j \ll |\nu_n - \nu_j|$ for $j \neq n$, $\tilde{H}_{\rm int}(t) \approx \frac{1}{4} b_n e^{i(\alpha_n - \theta_n)}\sigma_+ + \mathrm{H.c.}$ picks up the signal only at the frequency ν_n.

As exemplified in Fig. 3(a), the heterodyne sensing using the CPMG sequences produces multiple dips at $1/(2\tau) = \pm(\nu_j - \omega_q)/k$ $(k = 1, 3, 5, \ldots)$, which implies ambiguous sensor responses especially when $\{\nu_j\}$ happen to be close to the qubit frequency ω_q. In contrast, our geodesic driving gives clear signal dips for accurate determination of all the signal frequencies, see Fig. 3(b). Our method is also more resilient to dephasing noise (Fig. 3) and is more robust against control errors (Fig. 4). The robustness can be further enhanced by combining composite pulse techniques

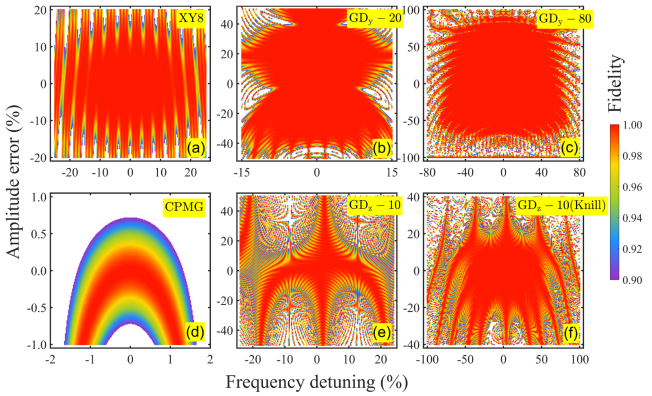

FIG. 4. Control fidelity with respect to amplitude and detuning errors for (a) XY8 sequence, (b) GD_y with $N = 20$, (c) GD_y with $N = 80$, (d) CPMG sequence with 40 pulses for heterodyne sensing, (e) GD_z with $N = 10$, (f) GD_z with $N = 10$ but each pulse is replaced by a Knill pulse. All the protocols have the same sequence time length, and the ideal Rabi frequency of the control is $2\pi \times 50$ MHz.

[see Fig. 4(e) for the result where each pulse is replaced by a Knill pulse [71,86,89]].

Conclusion.—We propose a quantum sensing scheme based on a quantum adiabatic shortcut along a geodesic path. This scheme offers the capability to resolve complex broadband signals and addresses the issues of spectral overlap and spurious signals that arise in existing DD-based quantum sensing methods. Notably, our approach allows for arbitrary frequency resolution through the utilization of synchronized readout techniques. Moreover, it exhibits robustness against control errors and effectively suppresses unwanted decoherence noise, making our protocol easy to be realized in experiments. The versatility of our method extends beyond signal detection; it can also be employed for the detection and control of various quantum objects, including single nuclear spins, spin clusters, and mechanical oscillators. Furthermore, our scheme holds promise for applications aimed at mitigating crosstalk in qubit arrays. In summary, our proposed quantum sensing scheme based on a quantum adiabatic shortcut along a geodesic path provides a universal solution for accurate signal detection, offering improved performance over existing methods. Its potential applications encompass a wide range of quantum systems and address key challenges in the field.

This work was supported by National Natural Science Foundation of China (Grant No. 12074131), the Natural Science Foundation of Guangdong Province (Grant No. 2021A1515012030), the ERC Synergy grant HyperQ (Grant No. 856432), the EU project C-QuENS (Grant No. 101135359), and the BMBF Zukunftscluster QSense: Quantensenoren für die biomedizinische Diagnostik (QMED) (Grant No. 03ZU1110FF).

*zhenyu.wang@m.scnu.edu.cn

[1] J. Preskill, Quantum computing in the NISQ era and beyond, Quantum **2**, 79 (2018).
[2] E. Paladino, Y. M. Galperin, G. Falci, and B. L. Altshuler, 1/f noise: Implications for solid-state quantum information, Rev. Mod. Phys. **86**, 361 (2014).
[3] C. L. Degen, F. Reinhard, and P. Cappellaro, Quantum sensing, Rev. Mod. Phys. **89**, 035002 (2017).
[4] J. F. Barry, J. M. Schloss, E. Bauch, M. J. Turner, C. A. Hart, L. M. Pham, and R. L. Walsworth, Sensitivity optimization for NV-diamond magnetometry, Rev. Mod. Phys. **92**, 015004 (2020).
[5] L. Viola, E. Knill, and S. Lloyd, Dynamical decoupling of open quantum systems, Phys. Rev. Lett. **82**, 2417 (1999).
[6] W. Yang, Z.-Y. Wang, and R.-B. Liu, Preserving qubit coherence by dynamical decoupling, Front. Phys. **6**, 2 (2011).
[7] C. Munuera-Javaloy, R. Puebla, and J. Casanova, Dynamical decoupling methods in nanoscale NMR, Europhys. Lett. **134**, 30001 (2021).
[8] M. W. Doherty, N. B. Manson, P. Delaney, F. Jelezko, J. Wrachtrup, and L. C. L. Hollenberg, The nitrogen-vacancy colour centre in diamond, Phys. Rep. **528**, 1 (2013).
[9] Y. Wu, F. Jelezko, M. B. Plenio, and T. Weil, Diamond quantum devices in biology, Angew. Chem., Int. Ed. Engl. **55**, 6586 (2016).
[10] J. R. Weber, W. F. Koehl, J. B. Varley, A. Janotti, B. B. Buckley, C. G. Van de Walle, and D. D. Awschalom, Quantum computing with defects, Proc. Natl. Acad. Sci. U.S.A. **107**, 8513 (2010).
[11] S. Kolkowitz, Q. P. Unterreithmeier, S. D. Bennett, and M. D. Lukin, Sensing distant nuclear spins with a single electron spin, Phys. Rev. Lett. **109**, 137601 (2012).
[12] N. Zhao, J. Honert, B. Schmid, M. Klas, J. Isoya, M. Markham, D. Twitchen, F. Jelezko, R. B. Liu, H. Fedder, and J. Wrachtrup, Sensing single remote nuclear spins, Nat. Nanotechnol. **7**, 657 (2012).
[13] T. Staudacher, F. Shi, S. Pezzagna, J. Meijer, J. Du, C. A. Meriles, F. Reinhard, and J. Wrachtrup, Nuclear magnetic resonance spectroscopy on a (5-Nanometer)^3 sample volume, Science **339**, 561 (2013).
[14] C. Müller, X. Kong, J.-M. Cai, K. Melentijević, A. Stacey, M. Markham, D. Twitchen, J. Isoya, S. Pezzagna, J. Meijer, J. Du, M. B. Plenio, B. Naydenov, L. P. McGuinness, and F. Jelezko, Nuclear magnetic resonance spectroscopy with single spin sensitivity, Nat. Commun. **5**, 4703 (2014).
[15] D. Rugar, H. J. Mamin, M. H. Sherwood, M. Kim, C. T. Rettner, K. Ohno, and D. D. Awschalom, Proton magnetic resonance imaging using a nitrogen-vacancy spin sensor, Nat. Nanotechnol. **10**, 120 (2015).
[16] S. J. DeVience, L. M. Pham, I. Lovchinsky, A. O. Sushkov, N. Bar-Gill, C. Belthangady, F. Casola, M. Corbett, H. Zhang, M. Lukin, H. Park, A. Yacoby, and R. L. Walsworth, Nanoscale NMR spectroscopy and imaging of multiple nuclear species, Nat. Nanotechnol. **10**, 129 (2015).
[17] D. R. Glenn, D. B. Bucher, J. Lee, M. D. Lukin, H. Park, and R. L. Walsworth, High-resolution magnetic resonance spectroscopy using a solid-state spin sensor, Nature (London) **555**, 351 (2018).
[18] J. E. Lang, J. Casanova, Z.-Y. Wang, M. B. Plenio, and T. S. Monteiro, Enhanced resolution in nanoscale NMR via quantum sensing with pulses of finite duration, Phys. Rev. Appl. **7**, 054009 (2017).
[19] M. Pfender, P. Wang, H. Sumiya, S. Onoda, W. Yang, D. B. R. Dasari, P. Neumann, X.-Y. Pan, J. Isoya, R.-B. Liu, and J. Wrachtrup, High-resolution spectroscopy of single nuclear spins via sequential weak measurements, Nat. Commun. **10**, 594 (2019).
[20] D. B. Bucher, D. P. L. Aude Craik, M. P. Backlund, M. J. Turner, O. Ben Dor, D. R. Glenn, and R. L. Walsworth, Quantum diamond spectrometer for nanoscale NMR and ESR spectroscopy, Nat. Protoc. **14**, 2707 (2019).
[21] J. Casanova, E. Torrontegui, M. B. Plenio, J. J. García-Ripoll, and E. Solano, Modulated continuous wave control for energy-efficient electron-nuclear spin coupling, Phys. Rev. Lett. **122**, 010407 (2019).
[22] N. Aharon, I. Schwartz, and A. Retzker, Quantum control and sensing of nuclear spins by electron spins under power limitations, Phys. Rev. Lett. **122**, 120403 (2019).

[23] C. Munuera-Javaloy, Y. Ban, X. Chen, and J. Casanova, Robust detection of high-frequency signals at the nanoscale, Phys. Rev. Appl. **14**, 054054 (2020).
[24] J. Cerrillo, S. Oviedo Casado, and J. Prior, Low field nano-NMR via three-level system control, Phys. Rev. Lett. **126**, 220402 (2021).
[25] J. Meinel, V. Vorobyov, P. Wang, B. Yavkin, M. Pfender, H. Sumiya, S. Onoda, J. Isoya, R.-B. Liu, and J. Wrachtrup, Quantum nonlinear spectroscopy of single nuclear spins, Nat. Commun. **13**, 5318 (2022).
[26] P. Wang, W. Yang, and R. Liu, Using weak measurements to synthesize projective measurement of nonconserved observables of weakly coupled nuclear spins, Phys. Rev. Appl. **19**, 054037 (2023).
[27] C. Munuera-Javaloy, A. Tobalina, and J. Casanova, High-resolution NMR spectroscopy at large fields with nitrogen vacancy centers, Phys. Rev. Lett. **130**, 133603 (2023).
[28] F. Shi, Q. Zhang, P. Wang, H. Sun, J. Wang, X. Rong, M. Chen, C. Ju, F. Reinhard, H. Chen, J. Wrachtrup, J. Wang, and J. Du, Single-protein spin resonance spectroscopy under ambient conditions, Science **347**, 1135 (2015).
[29] I. Lovchinsky, A. O. Sushkov, E. Urbach, N. P. de Leon, S. Choi, K. De Greve, R. Evans, R. Gertner, E. Bersin, C. Müller, L. McGuinness, F. Jelezko, R. L. Walsworth, H. Park, and M. D. Lukin, Nuclear magnetic resonance detection and spectroscopy of single proteins using quantum logic, Science **351**, 836 (2016).
[30] C. Munuera-Javaloy, R. Puebla, B. D. Anjou, M. B. Plenio, and J. Casanova, Detection of molecular transitions with nitrogen-vacancy centers and electron-spin labels, npj Quantum Inf. **8**, 140 (2022).
[31] N. Zhao, J.-L. Hu, S.-W. Ho, J. T. K. Wan, and R. B. Liu, Atomic-scale magnetometry of distant nuclear spin clusters via nitrogen-vacancy spin in diamond, Nat. Nanotechnol. **6**, 242 (2011).
[32] F. Shi, X. Kong, P. Wang, F. Kong, N. Zhao, R. B. Liu, and J. Du, Sensing and atomic-scale structure analysis of single nuclear-spin clusters in diamond, Nat. Phys. **10**, 21 (2014).
[33] J. E. Lang, R. B. Liu, and T. S. Monteiro, Dynamical decoupling-based quantum sensing: Floquet spectroscopy, Phys. Rev. X **5**, 041016 (2015).
[34] Z.-Y. Wang, J. F. Haase, J. Casanova, and M. B. Plenio, Positioning nuclear spins in interacting clusters for quantum technologies and bioimaging, Phys. Rev. B **93**, 174104 (2016).
[35] K. Sasaki, K. M. Itoh, and E. Abe, Determination of the position of a single nuclear spin from free nuclear precessions detected by a solid-state quantum sensor, Phys. Rev. B **98**, 121405(R) (2018).
[36] J. Zopes, K. S. Cujia, K. Sasaki, J. M. Boss, K. M. Itoh, and C. L. Degen, Three-dimensional localization spectroscopy of individual nuclear spins with sub-Angstrom resolution, Nat. Commun. **9**, 4678 (2018).
[37] J. Zopes, K. Herb, K. S. Cujia, and C. L. Degen, Three dimensional nuclear spin positioning using coherent radio-frequency control, Phys. Rev. Lett. **121**, 170801 (2018).
[38] M. H. Abobeih, J. Randall, C. E. Bradley, H. P. Bartling, M. A. Bakker, M. J. Degen, M. Markham, D. J. Twitchen, and T. H. Taminiau, Atomic-scale imaging of a 27-nuclear-spin cluster using a quantum sensor, Nature (London) **576**, 411 (2019).
[39] K. S. Cujia, K. Herb, J. Zopes, J. M. Abendroth, and C. L. Degen, Parallel detection and spatial mapping of large nuclear spin clusters, Nat. Commun. **13**, 1260 (2022).
[40] L. T. Hall, J. H. Cole, C. D. Hill, and L. C. L. Hollenberg, Sensing of fluctuating nanoscale magnetic fields using nitrogen-vacancy centers in diamond, Phys. Rev. Lett. **103**, 220802 (2009).
[41] A. Laraoui, J. S. Hodges, and C. A. Meriles, Magnetometry of random ac magnetic fields using a single nitrogen-vacancy center, Appl. Phys. Lett. **97**, 143104 (2010).
[42] A. Z. Chaudhry, Utilizing nitrogen-vacancy centers to measure oscillating magnetic fields, Phys. Rev. A **90**, 042104 (2014).
[43] A. Z. Chaudhry, Detecting the presence of weak magnetic fields using nitrogen-vacancy centers, Phys. Rev. A **91**, 062111 (2015).
[44] S. Schmitt, T. Gefen, F. M. Stürner, T. Unden, G. Wolff, C. Müller, J. Scheuer, B. Naydenov, M. Markham, S. Pezzagna, J. Meijer, I. Schwarz, M. Plenio, A. Retzker, L. P. McGuinness, and F. Jelezko, Submillihertz magnetic spectroscopy performed with a nanoscale quantum sensor, Science **356**, 832 (2017).
[45] J. M. Boss, K. S. Cujia, J. Zopes, and C. L. Degen, Quantum sensing with arbitrary frequency resolution, Science **356**, 837 (2017).
[46] T. Joas, A. M. Waeber, G. Braunbeck, and F. Reinhard, Quantum sensing of weak radio-frequency signals by pulsed Mollow absorption spectroscopy, Nat. Commun. **8**, 964 (2017).
[47] A. Stark, N. Aharon, T. Unden, D. Louzon, A. Huck, A. Retzker, U. L. Andersen, and F. Jelezko, Narrow-bandwidth sensing of high-frequency fields with continuous dynamical decoupling, Nat. Commun. **8**, 1105 (2017).
[48] Y. Chu, P. Yang, M. Gong, M. Yu, B. Yu, M. B. Plenio, A. Retzker, and J. Cai, Precise spectroscopy of high-frequency oscillating fields with a single-qubit sensor, Phys. Rev. Appl. **15**, 014031 (2021).
[49] J. Meinel, V. Vorobyov, B. Yavkin, D. Dasari, H. Sumiya, S. Onoda, J. Isoya, and J. Wrachtrup, Heterodyne sensing of microwaves with a quantum sensor, Nat. Commun. **12**, 2737 (2021).
[50] G. Wang, Y.-X. Liu, J. M. Schloss, S. T. Alsid, D. A. Braje, and P. Cappellaro, Sensing of arbitrary-frequency fields using a quantum mixer, Phys. Rev. X **12**, 021061 (2022).
[51] Z. Jiang, H. Cai, R. Cernansky, X. Liu, and W. Gao, Quantum sensing of radio-frequency signal with NV centers in SiC, Sci. Adv. **9**, eadg2080 (2023).
[52] T. H. Taminiau, J. J. T. Wagenaar, T. van der Sar, F. Jelezko, V. V. Dobrovitski, and R. Hanson, Detection and control of individual nuclear spins using a weakly coupled electron spin, Phys. Rev. Lett. **109**, 137602 (2012).
[53] Z.-Y. Wang, J. Casanova, and M. B. Plenio, Delayed entanglement echo for individual control of a large number of nuclear spins, Nat. Commun. **8**, 14660 (2017).
[54] J. F. Haase, Z.-Y. Wang, J. Casanova, and M. B. Plenio, Soft quantum control for highly selective interactions among joint quantum systems, Phys. Rev. Lett. **121**, 050402 (2018).

[55] M. A. Perlin, Z.-Y. Wang, J. Casanova, and M. B. Plenio, Noise-resilient architecture of a hybrid electron-nuclear quantum register in diamond, Quantum Sci. Technol. **4**, 015007 (2019).
[56] S. S. Hegde, J. Zhang, and D. Suter, Efficient quantum gates for individual nuclear spin qubits by indirect control, Phys. Rev. Lett. **124**, 220501 (2020).
[57] H. P. Bartling, M. H. Abobeih, B. Pingault, M. J. Degen, S. J. H. Loenen, C. E. Bradley, J. Randall, M. Markham, D. J. Twitchen, and T. H. Taminiau, Entanglement of spin-pair qubits with intrinsic dephasing times exceeding a minute, Phys. Rev. X **12**, 011048 (2022).
[58] J. Casanova, Z.-Y. Wang, and M. B. Plenio, Noise-resilient quantum computing with a nitrogen-vacancy center and nuclear spins, Phys. Rev. Lett. **117**, 130502 (2016).
[59] S. Pezzagna and J. Meijer, Quantum computer based on color centers in diamond, Appl. Phys. Rev. **8**, 011308 (2021).
[60] J. Cai, A. Retzker, F. Jelezko, and M. B. Plenio, A largescale quantum simulator on a diamond surface at room temperature, Nat. Phys. **9**, 168 (2013).
[61] L. Childress and R. Hanson, Diamond NV centers for quantum computing and quantum networks, MRS Bull. **38**, 134 (2013).
[62] N. Kalb, A. A. Reiserer, P. C. Humphreys, J. J. W. Bakermans, S. J. Kamerling, N. H. Nickerson, S. C. Benjamin, D. J. Twitchen, M. Markham, and R. Hanson, Entanglement distillation between solid-state quantum network nodes, Science **356**, 928 (2017).
[63] P. C. Humphreys, N. Kalb, J. P. J. Morits, R. N. Schouten, R. F. L. Vermeulen, D. J. Twitchen, M. Markham, and R. Hanson, Deterministic delivery of remote entanglement on a quantum network, Nature (London) **558**, 268 (2018).
[64] M. Pompili, S. L. N. Hermans, S. Baier, H. K. C. Beukers, P. C. Humphreys, R. N. Schouten, R. F. L. Vermeulen, M. J. Tiggelman, L. dos Santos Martins, B. Dirkse, S. Wehner, and R. Hanson, Realization of a multinode quantum network of remote solid-state qubits, Science **372**, 259 (2021).
[65] H. Y. Carr and E. M. Purcell, Effects of diffusion on free precession in nuclear magnetic resonance experiments, Phys. Rev. **94**, 630 (1954).
[66] S. Meiboom and D. Gill, Modified spin-echo method for measuring nuclear relaxation times, Rev. Sci. Instrum. **29**, 688 (1958).
[67] T. Gullion, D. B. Baker, and M. S. Conradi, New, compensated Carr-Purcell sequences, J. Magn. Reson. **89**, 479 (1990).
[68] M. Loretz, J. M. Boss, T. Rosskopf, H. J. Mamin, D. Rugar, and C. L. Degen, Spurious harmonic response of multipulse quantum sensing sequences, Phys. Rev. X **5**, 021009 (2015).
[69] V. M. Frey, S. Mavadia, L. M. Norris, W. de Ferranti, D. Lucarelli, L. Viola, and M. J. Biercuk, Application of optimal band-limited control protocols to quantum noise sensing, Nat. Commun. **8**, 2189 (2017).
[70] N. Zhao, J. Wrachtrup, and R.-B. Liu, Dynamical decoupling design for identifying weakly coupled nuclear spins in a bath, Phys. Rev. A **90**, 032319 (2014).
[71] J. Casanova, Z.-Y. Wang, J. F. Haase, and M. B. Plenio, Robust dynamical decoupling sequences for individual nuclear-spin addressing, Phys. Rev. A **92**, 042304 (2015).
[72] Z.-Y. Wang, J. E. Lang, S. Schmitt, J. Lang, J. Casanova, L. McGuinness, T. S. Monteiro, F. Jelezko, and M. B. Plenio, Randomization of pulse phases for unambiguous and robust quantum sensing, Phys. Rev. Lett. **122**, 200403 (2019).
[73] Z.-Y. Wang, J. Casanova, and M. B. Plenio, Enhancing the robustness of dynamical decoupling sequences with correlated random phases, Symmetry **12**, 730 (2020).
[74] Z.-Y. Wang and M. B. Plenio, Necessary and sufficient condition for quantum adiabatic evolution by unitary control fields, Phys. Rev. A **93**, 052107 (2016).
[75] K. Xu, T. Xie, F. Shi, Z.-Y. Wang, X. Xu, P. Wang, Y. Wang, M. B. Plenio, and J. Du, Breaking the quantum adiabatic speed limit by jumping along geodesics, Sci. Adv. **5**, eaax3800 (2019).
[76] Y. Liu and Z.-Y. Wang, Shortcuts to adiabaticity with inherent robustness and without auxiliary control, arXiv: 2211.02543.
[77] M. Gong, M. Yu, R. Betzholz, Y. Chu, P. Yang, Z. Wang, and J. Cai, Accelerated quantum control in a three-level system by jumping along the geodesics, Phys. Rev. A **107**, L040602 (2023).
[78] M. V. Berry, Transitionless quantum driving, J. Phys. A **42**, 365303 (2009).
[79] D. Géury-Odelin, A. Ruschhaupt, A. Kiely, E. Torrontegui, S. Marínez-Garaot, and J. G. Muga, Shortcuts to adiabaticity: Concepts, methods, and applications, Rev. Mod. Phys. **91**, 045001 (2019).
[80] D. Chruscinski and A. Jamiolkowski, *Geometric Phases in Classical and Quantum Mechanics* (Birkhäuser, Boston, 2004).
[81] See Supplemental Material at http://link.aps.org/supplemental/10.1103/PhysRevLett.132.250801, which includes Refs. [82–84], for simulation details and additional information about the spectral responses in quantum sensing.
[82] J.-M. Cai, B. Naydenov, R. Pfeiffer, L. P. McGuinness, K. D. Jahnke, F. Jelezklo, M. B. Plenio, and A. Retzker, Robust dynamical decoupling with concatenated continuous driving, New J. Phys. **14**, 113023 (2012).
[83] C. Gardiner, *Handbook of Stochastic Methods for Physics, Chemistry, and the Natural Sciences* (Springer-Verlag, Berlin, 2004), Chap. 3.
[84] X. Wang, C.-S. Yu, and X. X. Yi, An alternative quantum fidelity for mixed states of qudits, Phys. Lett. A **373**, 58 (2008).
[85] Ł. Cywiński, R. M. Lutchyn, C. P. Nave, and S. Das Sarma, How to enhance dephasing time in superconducting qubits, Phys. Rev. B **77**, 174509 (2008).
[86] C. A. Ryan, J. S. Hodges, and D. G. Cory, Robust decoupling techniques to extend quantum coherence in diamond, Phys. Rev. Lett. **105**, 200402 (2010).
[87] G. T. Genov, D. Schraft, N. V. Vitanov, and T. Halfmann, Arbitrarily accurate pulse sequences for robust dynamical decoupling, Phys. Rev. Lett. **118**, 133202 (2017).
[88] G. A. Alvarez and D. Suter, Measuring the spectrum of colored noise by dynamical decoupling, Phys. Rev. Lett. **107**, 230501 (2011).
[89] R. Tycko and A. Pines, Iterative schemes for broad-band and narrow-band population inversion in NMR, Chem. Phys. Lett. **111**, 462 (1984).